

A general theory of two-dimensional melting: the Gaussian-core model explained

Alejandro Mendoza-Coto,^{1,2,*} Valéria Mattiello,¹ Rômulo Cenci,¹ Nicolò Defenu,³ and Lucas Nicolao¹

¹*Departamento de Física, Universidade Federal de Santa Catarina, 88040-900 Florianópolis, Brazil*

²*Max-Planck-Institut für Physik komplexer Systeme, Nöthnitzer Str. 38, 01187 Dresden, Germany*

³*Institut für Theoretische Physik, Eidgenössische Technische Hochschule Zürich, 8093 Zürich, Switzerland*

(Dated: September 8, 2022)

A general theory for the melting of two dimensional solids explaining the variety of scenarios observed in different kind of models is up to date an open problem. Although the celebrated KTHNY theory have been able to predict the critical properties of the melting transition in a variety cases, it is already known that it is not able to capture the occurrence of first order transitions observed in certain systems. Moreover the analytical determination of non-universal quantities like the melting temperature within this theory remains widely open. In the present work we have developed a method that combines Self Consistent Variational Approximation with the Renormalization Group in order to deal simultaneously with the phonon fluctuations and the topological defects present in the melting process of two dimensional crystals. The method was applied with impressive success to the study of the phase diagram of the Gaussian-core model, capturing not only the reentrant feature of its 2D solid phase, but also the related critical temperatures as a function of the density in quantitative detail. The developed method can be directly applied to study the melting of any hexagonal simple crystal formed by particles interacting through any finite pairwise interaction potential. Additionally, it has the potential to explain the occurrence of first order transitions in the melting process of two dimensional crystals.

Introduction.—Two dimensional systems described by continuous microscopic variables present unusual phase transitions between the low and high temperature phases. This is related with the fact that in two dimensions thermal fluctuations are quite strong, preventing the stabilization of a long range ordered phase [1–4]. In this scenario, a vestigial quasi long-range order is often observed at low temperatures with slowly power law decaying correlations functions [5, 6]. Such is the case of the nematic, 2D-solid and hexatic phases [7–15] in a vast class of different physical systems like ultra-thin magnetic films [16–18], quasi two dimensional copolymer systems [19, 20]), vortex matter in two dimensional superconductors [21–23] and many others [13, 14].

The study of these kind of phases has its origin in a series of pioneering works by Berezinskii, Kosterlitz, Thouless (BKT), Halperin, Nelson and Young [5, 6, 24–29]. In these works it was established the central role of the thermal induced process of pair unbinding and proliferation of topological defects in the disruption of the quasi long-range order. From the technical point of view the development of this research area is historically tied with the development of a proper Renormalization Group (RG) theory capable to describe the proliferation of the topological excitations at high-temperature. The success of this RG scheme granted the 2016 Nobel prize in physics [30].

Despite this huge success, important questions remain open today in the physics of 2D transitions. Most of these questions originate from the difficulty to properly estimate non-universal properties, such as the transition temperature, in the wide range of diverse physical system, where topological defects unbinding occurs. Indeed, while the BKT RG scheme yields a phenomenological description of the coarse grained topological variables, the connection between their properties and the actual microscopic theory at hand is often unfeasible. Thus, a natural question arises “How can we maintain a close

connection between the microscopic details of the system and its BKT description?”. In the context of the melting of two-dimensional crystals, one can also ask “How can we construct a RG scheme which accounts for the variety of scenarios observed in simulations and experiments that include first order phase transitions [31–34]?”. The answer to this second question is the topic of the present work.

In order to access non-universal properties, first, it is necessary to build RG equations maintaining full connection with the microscopic model. Second, good estimates of the relevant energy of the defects are needed to capture the temperature scale of the corresponding phase transition [35, 36]. And lastly, the effects of smooth fluctuations on the ground state should be taken into account, since close to the melting temperature they could produce a significant deviation of the effective microscopic rigidity from its bare or zero temperature value [6, 17, 37]. Following this route it has been possible to estimate the properties of the topological phase transition in diverse XY model configurations [36, 38–41]. In few specific cases the Self-Consistent Harmonic Approximation (SCHA) has been used to calculate the effective rigidity as a function of temperature and simultaneously this information used as an input of the RG equations in order to estimate the melting temperature better than RG or variational Mean Field alone [35, 40].

In this context, the construction of a similar calculation scheme for the study of the melting process of two dimensional crystals still constitutes an unexplored route. The construction of such method shall provide not only good estimates for the melting temperature of two dimensional crystals but shall also yield a self-consistent approach providing the correct qualitative behavior of the phases below and above the transition. This last property constitutes a substantial advantage with respect to the several implementations of Density Functional Theory (DFT), which have been used to tackle the

melting problem in two dimensional crystals,[42, 43]. These traditional approaches in the vast majority of cases consider that the 2D solid phase can be treated as a periodic phase which breaks translational symmetry, yielding a major shortcoming that in general produces a wrong description of the critical properties of the melting transition, or even predict incorrectly the nature of the phase transition itself. In light of the previous discussion, a theory of 2D melting, that we intend to construct, represents a major advancement towards the understanding of melting in two-dimensional crystals, as it will be capable to explain the diversity of melting scenarios observed in numerical simulations [31–34, 44–48].

In this work we implement a Self-Consistent Harmonic technique that retains total connection with the microscopic model. This allows us to determine the effective elastic Lamé’s coefficients as a function of the density of particles and the temperature. A first mean field estimate of the melting temperature then can be found as the moment when the effective transversal elastic rigidity goes to zero. Contrasting with all other DFT techniques in two dimensions, this kind of mean field calculation has the distinctive virtue of being able to describe properly the qualitative behavior of the phases below and above the melting transition. To improve the mean field results, we use the obtained values for the effective elastic coefficients as an input into the RG equations for the melting transition of a two-dimensional solid. This produces a strong correction to the phase boundary of the 2D solid phase. To test the quality of this method that incorporates the SCHA into the RG theory we performed extensive overdamped Langevin simulations to determine an accurate melting curve for the two dimensional solid phase. The obtained analytical results shows an impressive agreement with the simulational results.

Model and Methods.—We consider a classical system of particles in two dimensions interacting through a Gaussian pairwise potential of the form $V(r) = V_0 \exp(-r^2/r_0^2)$, known as the Gaussian-Core Model (GCM) [49–51]. The parameters r_0 and V_0 represent the range and the intensity of our soft-core potential, respectively. The partition function of this model can be written directly in terms of the configurational integral, which is obtained after integrating over all momenta of the particles:

$$Z = \frac{1}{N!} \int \left(\prod_i \frac{d^2 \mathbf{r}_i}{\Lambda^2} \right) e^{-\beta \sum_{i < j} V(|\mathbf{r}_i - \mathbf{r}_j|)}, \quad (1)$$

where $\Lambda \equiv h/\sqrt{2\pi m k_B T}$ is the de Broglie thermal wave length and N the number of particles. Having in mind that our goal is to study the melting of the two-dimensional solid phase it is natural to consider that each particle will effectively explore a region of finite "volume" around its equilibrium position. This consideration allows us to write the position of each particle \mathbf{r}_i as $\mathbf{R}_i + \mathbf{u}_i$, where \mathbf{R}_i represent the equilibrium lattice position of the i -particle and \mathbf{u}_i its relative position respect \mathbf{R}_i . In this way, once we include the combinatorial factor of distributing the N particles of the system on the N sites of

the solid, the partition function can be rewritten as:

$$Z = \int \prod_i \frac{d^2 \mathbf{u}_i}{\Lambda^2} e^{-\frac{\beta}{2} \sum_{i \neq j} V(|\mathbf{R}_i - \mathbf{R}_j + \mathbf{u}_i - \mathbf{u}_j|)}. \quad (2)$$

This last expression allows us to define our effective Hamiltonian as $H \equiv 1/2 \sum_{i \neq j} V(|\mathbf{R}_i - \mathbf{R}_j + \mathbf{u}_i - \mathbf{u}_j|)$. To calculate the melting curve we will implement a two-step procedure, firstly we use the Self-Consistent Harmonic Approximation to determine the effective Lamé’s elastic coefficients in the presence of phonon’s fluctuations. In a second step, the mean field melting curve can be improved using the values of the effective elastic coefficients as an input for the calculation of the bare Frank constant and fugacity in the framework of the well known renormalization group theory for the defect mediated melting of the solid phase of two-dimensional solids [5, 6, 26, 52].

Before proceeding with the implementation of the SCHA is important to mention some well known properties of the model considered in this work. The GCM have a density versus temperature reentrant hexagonal solid phase in its low temperature regime [50] and the melting process of the solid phase occurs through a two-step process with an intermediate hexatic phase existing in a very narrow temperature region [51, 53].

We begin the implementation of our SCHA choosing our test Hamiltonian in the form:

$$H_0 = N \epsilon_0(\rho) + \frac{1}{2} \left(\frac{\sqrt{3} a^2(\rho)}{2} \right) \times \int_{BZ} \frac{d^2 q}{(2\pi)^2} \left[f_1(\mathbf{q}) |\hat{u}_{\parallel}(\mathbf{q})|^2 + f_2(\mathbf{q}) |\hat{u}_{\perp}(\mathbf{q})|^2 \right], \quad (3)$$

where $\epsilon_0(\rho)$ represent the ground state energy per particle of the GCM at a given density ρ and $a(\rho) = (2/\sqrt{3}\rho)^{1/2}$, represent the lattice spacing of the hexagonal lattice. The dispersion relations $f_1(\mathbf{q})$ and $f_2(\mathbf{q})$ represent the longitudinal and transversal elastic test response functions to be found, in principle, through the minimization of the variational free energy functional. Additionally, the longitudinal and transversal elastic fields are given as: $\hat{u}_{\parallel}(\mathbf{q}) = -i\mathbf{q} \cdot \hat{\mathbf{u}}(\mathbf{q})/q$ and $\hat{u}_{\perp}(\mathbf{q}) = -i\mathbf{q}_{\perp} \cdot \hat{\mathbf{u}}(\mathbf{q})/q$, with $\mathbf{q}_{\perp} = (-q_y, q_x)$.

Although the form of the test Hamiltonian may look highly elaborated it is in fact quite intuitive since it coincides with the expansion of H up to second order in powers of $\hat{\mathbf{u}}(\mathbf{q})$, considering generic dispersion relations for the longitudinal and transversal elastic modes. In the long wave limit ($q \rightarrow 0$), the harmonic theory predicts $f_1(\mathbf{q}) = (2\mu + \lambda)\mathbf{q}^2$ and $f_2(\mathbf{q}) = \mu\mathbf{q}^2$, where μ and λ represent the so-called Lamé’s elastic coefficients – these and other results of harmonic theory for the solid elasticity are reviewed in the Supplemental Material [53]. Finally, it is important to notice that since the field $\mathbf{u}(\mathbf{R}_i)$ is defined on the triangular lattice with spacing $a(\rho)$, the momentum integral in Eq. (3) is performed on the first Brillouin zone of such lattice, represented with the sub-index BZ along this work.

Now we can proceed with the construction of the variational free energy. As it is well known, the actual free energy of the system is bounded from above by the minimum of the functional:

$$F_{var} = F_0 + \langle H \rangle_0 - \langle H_0 \rangle_0, \quad (4)$$

where $\langle \circ \rangle_0 = \frac{1}{Z_0} \int \Pi_i d\mathbf{u}_i \exp(-\beta H_0) \circ$. Given the Gaussian character of our test model it is not hard to conclude that $\langle H_0 \rangle_0 = N\epsilon_0 + Nk_B T$, while the total free energy is given as:

$$F_0 = N\epsilon_0 + \frac{N}{\beta\rho} \int_{BZ} \frac{d^2q}{(2\pi)^2} \log \left[\frac{\beta\Lambda^2}{2\pi} \sqrt{f_1(\mathbf{q})f_2(\mathbf{q})} \right]. \quad (5)$$

The calculation of the Gaussian path integral leading to F_0 is presented in our Supplemental Material [53]. Now we should proceed with the calculus of $\langle H \rangle_0$, if we consider the translational symmetry of the solid phase is possible to write:

$$\langle H \rangle_0 = \frac{N}{2} \sum_{\mathbf{R}_i \neq \mathbf{0}} \langle V(\mathbf{R}_i + \mathbf{u}(\mathbf{R}_i) - \mathbf{u}(\mathbf{0})) \rangle_0, \quad (6)$$

where $\{\mathbf{R}_i\}$ represent the vectors of the triangular lattice at a given density. at the same time, the average interaction energy between two particles linked to lattice sites separated by a vector \mathbf{R}_i is given by:

$$\langle V(\mathbf{R} + \mathbf{u}(\mathbf{R}) - \mathbf{u}(\mathbf{0})) \rangle_0 = \int \frac{d^2q}{(2\pi)^2} e^{i\mathbf{q}\cdot\mathbf{R}} g_{\mathbf{q}}(\mathbf{R}) \hat{V}(q), \quad (7)$$

where $g_{\mathbf{q}}(\mathbf{R}) \equiv \langle e^{i\mathbf{q}\cdot(\mathbf{u}(\mathbf{R}) - \mathbf{u}(\mathbf{0}))} \rangle_0$ represent the positional correlation function calculated with the Boltzmann measure of H_0 . After some straightforward algebra [53], we can prove that:

$$g_{\mathbf{q}}(\mathbf{R}) = \exp \left\{ -\frac{1}{\beta\rho} \int_{BZ} \frac{d^2k}{(2\pi)^2} (1 - \cos(\mathbf{k}\cdot\mathbf{R})) \left[\frac{(\mathbf{k}\cdot\mathbf{q})^2}{k^2} \frac{1}{f_1(\mathbf{k})} + \frac{(\mathbf{k}_\perp\cdot\mathbf{q})^2}{k^2} \frac{1}{f_2(\mathbf{k})} \right] \right\}. \quad (8)$$

This expression once inserted in Eq. (7) complete the construction of the variational free energy functional in terms of $f_1(\mathbf{q})$ and $f_2(\mathbf{q})$. Finally, it is worth noticing that in the calculus of the average interaction potential Eq. (7) we have used the standard form of the Fourier transform considering that the arguments of the functions $V(\mathbf{r})$ in this case are not restricted to a periodic lattice.

In this way, the variational free energy per particle in units of $k_B T$ can be written as:

$$\beta f_{var}[f_1(\mathbf{q}), f_2(\mathbf{q})] = \frac{1}{\rho} \int_{BZ} \frac{d^2q}{(2\pi)^2} \log \left[\frac{\beta\Lambda^2}{2\pi} \sqrt{f_1(\mathbf{q})f_2(\mathbf{q})} \right] - 1 + \frac{\beta}{2} \sum_{\mathbf{R}_j \neq \mathbf{0}} \int \frac{d^2q}{(2\pi)^2} e^{i\mathbf{q}\cdot\mathbf{R}_j} g_{\mathbf{q}}(\mathbf{R}_j) \hat{V}(q), \quad (9)$$

where $g_{\mathbf{q}}(\mathbf{R}_j)$ is given by Eq. (8). Once we minimize the variational free energy with respect to $f_1(\mathbf{q})$ and $f_2(\mathbf{q})$, we obtain a set of nonlinear integral equations for these functions. This set of equations cannot be easily solved in general form, however it is expected that in the low momentum regime $f_1(\mathbf{q})$ and $f_2(\mathbf{q})$ are proportional to q^2 . It is possible then to detect the melting transition by looking to the curvature of these functions at low momentum, which can be naturally related to the effective Lamé coefficients. This relation is given by $r_1 = \frac{1}{2} \partial^2 f_1(q_0) / \partial q_0^2 \equiv 2\mu(T) + \lambda(T)$ and $r_2 = \frac{1}{2} \partial^2 f_2(q_0) / \partial q_0^2 \equiv \mu(T)$. The set of equations for r_1 and r_2 is derived in the Supplemental Material [53].

In order to finally close this system of equations we naturally approximate $f_1(\mathbf{q})$ and $f_2(\mathbf{q})$ by its quadratic low momentum form in the expression of $g_{\mathbf{q}}(\mathbf{R})$ in Eq. (8). This procedure lead us to the conclusion that:

$$g_{\mathbf{q}}(\mathbf{R}) = \exp \left[-\omega_{\parallel}(\mathbf{R}) q_{\parallel}^2 - \omega_{\perp}(\mathbf{R}) q_{\perp}^2 \right], \quad (10)$$

where q_{\parallel} and q_{\perp} represent the components of \mathbf{q} parallel and perpendicular to \mathbf{R} , and the coefficients $\omega_{\parallel}(\mathbf{R})$ and $\omega_{\perp}(\mathbf{R})$ depend on r_1 and r_2 in the following way:

$$\omega_{\parallel}(\mathbf{R}) = \frac{1}{\beta\rho} \left(\frac{A_{\parallel}(\mathbf{R})}{r_1} + \frac{A_{\perp}(\mathbf{R})}{r_2} \right) \quad (11)$$

$$\omega_{\perp}(\mathbf{R}) = \frac{1}{\beta\rho} \left(\frac{A_{\perp}(\mathbf{R})}{r_1} + \frac{A_{\parallel}(\mathbf{R})}{r_2} \right).$$

The functions $A_{\parallel}(\mathbf{R})$ and $A_{\perp}(\mathbf{R})$ are given as integrals over the first Brillouin zone of the hexagonal lattice of a given function of \mathbf{R} , as derived in detail in the Supplemental Material [53]. The expression for $g_{\mathbf{q}}(\mathbf{R})$ in Eq. (10) complete our construction of the closed system of equations for r_1 and r_2 , which now could be use directly to study the melting process of the hexagonal solid phase within the SCHa for any kind of pair interaction potential with a well behaved $\hat{V}(q)$.

Results.—As mentioned earlier in this work we focus on the analytical study of the GCM for which $\hat{V}(q) = \pi V_0 e^{-q^2 r_0^2/4}$. The Gaussian form of this potential allows for some analytical advances in the numerical solution of the system of equations determining $r_1(T)$ and $r_2(T)$, as described in the Supplemental Material [53]. In Fig. 1 we show the numerical solution for $\mu(T)$ and $2\mu(T) + \lambda(T)$ for several particles densities in two dimensions. As we can see, the transversal elastic coefficient $\mu(T)$ displays the typical behavior of the order parameter in a BKT-like transition with and exponential behavior with temperature close to T_c . In terms of densities, we are able to observe the re-entrant behavior of $\mu(T)$ already expected from numerical simulations results [51]. In the other hand, the longitudinal elastic coefficient grows steadily increasing density, as expected for any stable solid. Additionally, we observe that $2\mu(T) + \lambda(T)$ display different kind of behaviors with temperature in the low and high density regimes. Finally, the melting curve in the temperature versus density plane, can be observe in Fig. (2) in green. As we can see the 2D solid phase presents the reentrant behavior well established in the litera-

ture for GCM in two dimensions. However, although the implemented method has the merit of being a novel mean field calculation describing properly the qualitative behavior of the phases involved in the melting transition, it has the drawback of overestimate significantly the maximum melting temperature of the model.

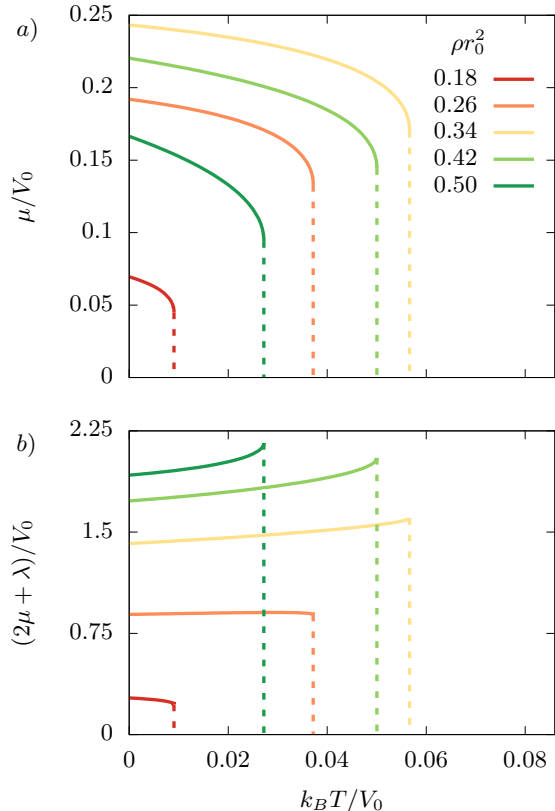


FIG. 1: Behaviour of the Lamé coefficients μ and $2\mu + \lambda$, resulting from the variational approach as function of the temperature, for some specific density values. The temperature ranges between zero and the critical value T_m , at which the $\mu(T)$ function has a infinite slope.

Defect mediated phase transition and RG relations.— The lack of agreement between the mean field results and the computational results is somewhat expected, since the mean field method implemented does not take into account the effects of the topological defects, called dislocations. The proliferation of dislocations is quite effective in disrupting the periodic order of the solid phase as the melting process occurs increasing temperature. The theory for describing the defect mediated melting transition in two dimensions, also known as KTHNY theory, was provided in a series of foundational works by Toner, Halperin, Nelson and Young [26, 28, 29, 52] in which RG equations are obtained for the renormalized Frank’s elastic constant and fugacity of the dislocations, respectively.

The RG system of equation for the Frank’s elastic constant

($K(l)$) and the defect’s fugacity ($y(l)$) is given by:

$$\begin{aligned} \frac{dK^{-1}}{dl} &= \frac{3}{2}\pi y^2(l)e^{K(l)/8\pi} \left[I_0\left(\frac{K(l)}{8\pi}\right) - \frac{1}{2}I_1\left(\frac{K(l)}{8\pi}\right) \right], \\ \frac{dy}{dl} &= \left[2 - \frac{K(l)}{8\pi} \right] y(l) + 2\pi y^2(l)e^{K(l)/16\pi} I_0\left(\frac{K(l)}{8\pi}\right), \end{aligned} \quad (12)$$

with the initial conditions given the bare values of K/k_bT and y , i.e. $K(0) = \frac{4\mu(\mu+\lambda)}{(2\mu+\lambda)k_B T}$ and $y(0) = \exp(-E_c/k_B T)$. Here μ and λ represent the Lamé’s coefficients and E_c represent the energy of an isolated defect. Within RG theory the melting temperature corresponds to the lowest temperature at which $K(l \rightarrow +\infty) = 0$, signaling that the long distance effective rigidity of the system goes to zero.

To use the RG equations for detecting the melting transition the energy of the relevant defects in the melting process should be provided. In our case we estimate such quantity using the harmonic elastic theory to calculate half of the energy corresponding to a pair of conjugate dislocations. The obtained result depends on the orientation of the Burguer’s vector of the dislocations (\mathbf{e}) respect to the underlying lattice and weakly on the orientation of the distance vector between the dislocations of the pair \mathbf{d} . Since there is a continuum of possible configurations for the dislocation pair the energy of the dislocation is estimated as the average energy between all configurations maintaining the minimum possible length of the dislocation pair. In this way the energy of a dislocation in units of $k_B T$ is estimated to be:

$$\begin{aligned} \frac{E_c}{k_B T} &= K(0) \int_{BZ} \frac{d^2 q}{(2\pi)^2} \frac{\langle (\mathbf{q}_\perp \cdot \mathbf{e})^2 \rangle \langle \sin(\mathbf{q} \cdot \mathbf{d}/2)^2 \rangle}{q^4} \\ &\approx 0.072K(0). \end{aligned} \quad (13)$$

An important consideration to reach this result is related to the minimum distance between a pair of stable dislocations. Numerical simulations performed for the GCM model lead us to the conclusion that such distance is higher than the lattice spacing. One useful way to obtain a pair of stable dislocations in this system is to subtract a particle from a perfect crystal configuration and leave the system to relax to a new stable configuration exhibiting a pair of dislocations separated by a distance that can be roughly estimated to $d = \sqrt{3}a$ [54]. More details on how to reach this conclusion and calculate the energy of a dislocation pair can be found in the Supplemental Material [53].

We realize now that since the initial condition of the RG flow equations are completely determined by the value of the bare Frank’s constant $K(0)$, the melting transition will occur at a certain specific value of the parameter $K(0)$. In this case the direct numerical solution of the system of Eqs. (12) allow us to conclude that the melting transition occurs approximately at $K(0)_c \approx 23.922\pi$ [65]. This value can now be used to build the melting curve considering the calculated Lamé’s coefficients, $\mu(T)$ and $\lambda(T)$, dressed by phonons fluctuations, which can be obtained from the solution of the equation

$4\mu(\rho, T)(\mu(\rho, T) + \lambda(\rho, T)) / ((2\mu(\rho, T) + \lambda(\rho, T))k_B T) = 23.922\pi$. The result of this procedure is shown in Fig. 2, to be compared with our Langevin dynamics simulations estimations for the 2D solid melting temperature, using system sizes consisting of up to $N = 8100$ particles – more details about the numerical simulations and their results can be found in the Supplemental Material [53]. The agreement between the analytical results and the computational results is quite impressive, indicating that the proposed scheme not only captures well the phenomenology of the described phase transition but also produce a precise description of the melting transition.

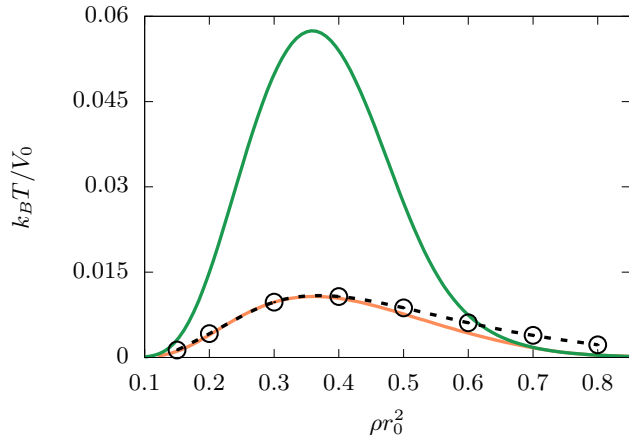


FIG. 2: Phase diagram for simulations are represented by black circles and dashed line (cubic splines used as guide to the eyes). The result for variational mean field is presented by a green line and renormalization group + variational approach in orange.

Conclusion.—In the present work we have developed a novel technique in order to study the melting transition of the two dimensional solid phase of the GCM. Although its melting phase diagram is already known from previous computational studies, up to our knowledge, this is the first time that this result is reproduced analytically with such level of accuracy. In contrast with other MF predictions, we have observed that the SCHA alone is able to predict correctly the qualitative properties of the melting transition, such as the reentrant melting curve and the density for which the melting temperature is higher. In spite of this, only the mechanism of topological defects proliferation related to BKT like transitions is able to explain the significant reduction of the melting temperature when compared with MF predictions. This mechanism is captured in our approach by performing a two-step calculation where the Franck’s elastic constant and the defects fugacity calculated by MF are used as initial condition of the RG flow describing vortex unbinding $K(0)$.

This approach demonstrates how the relative low value of the energy of dislocation pairs causes a drastic reduction of the melting temperature, due to the early proliferation of topological defect. The effect is correctly captured by the RG system in Eq. (12), once proper values of the defect parameters are introduced. Our estimate for the energy of the defects can be

seen as a leading order approximation, since in general it is expected that higher order contributions will depend on the particle’s density and on the Franck constant itself in a non-linear way. This is a possible explanation for the small difference observed in Fig. 2 between the analytical and numerical melting curves at higher densities. An improvement of the estimation of the energy of the defects is beyond the scope of the present work. Additionally, it is important to mention that in the low density regime where the effects of the phonon are weak we verified that, as expected, the melting curves calculated using the zero temperature Franck’s constant and using the effective one dressed by phonons produces similar melting curves.

We would like to stress that the presented method is an important step not only in the characterization of the melting transition of two 2D crystals but also to the study of this process in other modulated two dimensional systems, like magnetic 2D textures[55–59]. Finally, it is worth noticing that the developed method has the potential to produce melting scenarios originally not contained in the KTHNY theory. A first order transition melting scenario is in principle a possibility in those cases where the SCHA produces a discontinuous melting transition and the defect energy is high enough for the mean field transition to takes place at lower temperature than the one predicted by RG equations. In this sense, this kind of self-consistent variational plus RG methods can possibly provide a more general framework to explain the variety of melting scenarios observed in different kind of models.

Acknowledgement

AM-C acknowledges financial support from Fundação de Amparo à Pesquisa de Santa Catarina, Brazil (Fapesc). AM-C acknowledges hospitality and financial support from MIPKs. ND acknowledges useful discussions with G. Giachetti. This work is supported by the Deutsche Forschungsgemeinschaft (DFG, German Research Foundation) under Germany’s Excellence Strategy EXC2181/1-390900948 (the Heidelberg STRUCTURES Excellence Cluster).

Supplemental Material

A. Harmonic theory for the solid elasticity

The Hamiltonian of a classical system of N particles interacting through a pair potential:

$$\mathcal{H} = \sum_i \frac{\mathbf{p}_i^2}{2m} + \sum_{i<j} V(|\mathbf{r}_i - \mathbf{r}_j|), \quad (14)$$

and the associated canonical partition function:

$$Z_0 = \frac{1}{N!} \int \left(\prod_i \frac{d^2\mathbf{r}_i d^2\mathbf{p}_i}{h^2} \right) e^{-\beta\mathcal{H}} = \frac{1}{N!} \int \left(\prod_i \frac{d^2\mathbf{r}_i}{\Lambda^2} \right) e^{-\beta \sum_{i<j} V(|\mathbf{r}_i - \mathbf{r}_j|)}, \quad (15)$$

where $\Lambda \equiv h/\sqrt{2\pi mk_B T}$. Considering that at zero temperature particles are arranged in a triangular crystal with lattice sites \mathbf{R}_i , the fluctuations in the particles positions can be defined as $\mathbf{u}_i = \mathbf{r}_i - \mathbf{R}_i$. We can now expand the potential energy up to second order in \mathbf{u} :

$$\begin{aligned} V_0 &= \frac{1}{2} \sum_{i \neq j} V(|\mathbf{r}_i - \mathbf{r}_j|) = \frac{1}{2} \sum_{i \neq j} V(|\mathbf{R}_i - \mathbf{R}_j + \mathbf{u}_i - \mathbf{u}_j|) \\ &\approx \frac{1}{2} \sum_{i \neq j} \left\{ V(\mathbf{R}_i - \mathbf{R}_j) + \vec{\nabla} V(\mathbf{R}_i - \mathbf{R}_j) \cdot \Delta \mathbf{u} + \frac{1}{2} \Delta \mathbf{u}^T \cdot \mathbf{H} \cdot \Delta \mathbf{u} \right\}. \end{aligned} \quad (16)$$

Here $\Delta \mathbf{u} = \mathbf{u}_i - \mathbf{u}_j$ and \mathbf{H} represent the Hessian matrix of $V(\mathbf{R}_i - \mathbf{R}_j)$.

The Fourier transform on the triangular lattice is given by:

$$u(\mathbf{R}_j) = \frac{\sqrt{3}a^2}{2} \int_{BZ} \frac{d^2q}{(2\pi)^2} e^{i\mathbf{q} \cdot \mathbf{R}_j} \hat{u}(\mathbf{q}), \quad (17)$$

$$\hat{u}(\mathbf{q}) = \sum_j e^{-i\mathbf{q} \cdot \mathbf{R}_j} u(\mathbf{R}_j), \quad (18)$$

where $\mathbf{R}_j = a(n\mathbf{e}_1 + m\mathbf{e}_2)$, with n and m integers and $\mathbf{e}_1 = (1, 0)$ and $\mathbf{e}_2 = (-\frac{1}{2}, \frac{\sqrt{3}}{2})$, and the lattice spacing a as a function of density ρ is given by $a = (2/\sqrt{3}\rho)^{1/2}$. The momentum integral is performed over the first Brillouin zone (BZ) of the triangular lattice.

The linear term in eq. (16) vanishes by definition of the ground state. So, the interaction term in momentum space can be written as

$$\begin{aligned} V_0 &= N\epsilon_0 + \frac{1}{2} \frac{\sqrt{3}a^2}{2} \int_{BZ} \frac{d^2q}{(2\pi)^2} \left(2 \left(\frac{1}{2} \partial_x^2 V(R) \right)^{FT} (0) - 2 \left(\frac{1}{2} \partial_x^2 V(R) \right)^{FT} (\mathbf{q}) \right) \hat{u}_x(\mathbf{q}) \hat{u}_x(-\mathbf{q}) \\ &+ \frac{1}{2} \frac{\sqrt{3}a^2}{2} \int_{BZ} \frac{d^2q}{(2\pi)^2} \left(2 \left(\frac{1}{2} \partial_y^2 V(R) \right)^{FT} (0) - 2 \left(\frac{1}{2} \partial_y^2 V(R) \right)^{FT} (\mathbf{q}) \right) \hat{u}_y(\mathbf{q}) \hat{u}_y(-\mathbf{q}) \\ &+ \frac{1}{2} \frac{\sqrt{3}a^2}{2} \int_{BZ} \frac{d^2q}{(2\pi)^2} \left(2 (\partial_{xy} V(R))^{FT} (0) - 2 (\partial_{xy} V(R))^{FT} (\mathbf{q}) \right) \hat{u}_x(\mathbf{q}) \hat{u}_y(-\mathbf{q}), \end{aligned} \quad (19)$$

where ϵ_0 represent the ground state energy per particle of the system and $(F(\mathbf{R}))^{FT}(\mathbf{q}) \equiv \sum_j e^{i\mathbf{q} \cdot \mathbf{R}_j} F(\mathbf{R}_j)$. Using this property and expanding the exponential function up the second order in \mathbf{q} , we arrive at the well known elastic Hamiltonian for a two dimensional hexagonal solid:

$$\begin{aligned} V_0 &= N\epsilon_0 + \frac{1}{2} \frac{\sqrt{3}a^2}{2} \int_{BZ} \frac{d^2q}{(2\pi)^2} ((2\mu + \lambda)q_x^2 + \mu q_y^2) \hat{u}_x(\mathbf{q}) \hat{u}_x(-\mathbf{q}) \\ &+ \frac{1}{2} \frac{\sqrt{3}a^2}{2} \int_{BZ} \frac{d^2q}{(2\pi)^2} ((2\mu + \lambda)q_y^2 + \mu q_x^2) \hat{u}_y(\mathbf{q}) \hat{u}_y(-\mathbf{q}) \\ &+ \frac{1}{2} \frac{\sqrt{3}a^2}{2} \int_{BZ} \frac{d^2q}{(2\pi)^2} (2(\mu + \lambda)q_x q_y) \hat{u}_x(\mathbf{q}) \hat{u}_y(-\mathbf{q}). \end{aligned} \quad (20)$$

where the Lamé's coefficient (μ, λ) are given by the relations:

$$\begin{aligned}\mu &= \sum_{\mathbf{R} \neq 0} \left(\frac{R_y^2}{2} \right) \left(\frac{R_y^2 V'(R)}{R^3} + \frac{R_x^2 V''(R)}{R^2} \right), \\ 2\mu + \lambda &= \sum_{\mathbf{R} \neq 0} \left(\frac{R_x^2}{2} \right) \left(\frac{R_y^2 V'(R)}{R^3} + \frac{R_x^2 V''(R)}{R^2} \right).\end{aligned}\quad (21)$$

These are general relations that allow for the calculation of the elastic constants at zero temperature for a simple hexagonal crystal, once established the knowledge of $V(R)$.

Now we can proceed with the evaluation of the partition function in Eq.(15). To perform the functional integration over the configurations of $\hat{\mathbf{u}}(\mathbf{q})$ it is convenient to implement an orthogonal transformation to decouple the Cartesian components of $\hat{\mathbf{u}}(\mathbf{q})$. This is done introducing the longitudinal $\hat{u}_{\parallel}(\mathbf{q})$ and perpendicular $\hat{u}_{\perp}(\mathbf{q})$ components of the deformation field in the following way:

$$\begin{aligned}\hat{u}_x(\mathbf{q}) &= i \frac{q_x}{q} \hat{u}_{\parallel}(\mathbf{q}) - i \frac{q_y}{q} \hat{u}_{\perp}(\mathbf{q}), \\ \hat{u}_y(\mathbf{q}) &= i \frac{q_y}{q} \hat{u}_{\parallel}(\mathbf{q}) + i \frac{q_x}{q} \hat{u}_{\perp}(\mathbf{q}),\end{aligned}\quad (22)$$

And, as a consequence:

$$V_0 = N\epsilon_0 + \frac{1}{2} \left(\frac{\sqrt{3}a^2}{2} \right) \int_{BZ} \frac{d^2q}{(2\pi)^2} \left[f_1(q) |\hat{u}_{\parallel}(q)|^2 + f_2(q) |\hat{u}_{\perp}(q)|^2 \right], \quad (23)$$

where $f_1(q) = (2\mu + \lambda)q^2$ and $f_2(q) = \mu q^2$. After considering the combinatorial factor corresponding to the distribution the particles over the lattice sites, we can now rewrite our partition function as:

$$Z_0 = \int \prod_i \frac{d^2\mathbf{u}_i}{\Lambda^2} e^{-\beta V_0} = e^{-\beta N\epsilon_0} \left(\prod_q \frac{2\pi}{\beta\Lambda^2 \sqrt{f_1(q)f_2(q)}} \right). \quad (24)$$

It is straightforward to conclude that

$$\begin{aligned}F_0 &= -\frac{1}{\beta} \log Z_0 = N\epsilon_0 + \frac{1}{\beta} \sum_{\mathbf{q}} \log \left(\frac{\beta\Lambda^2}{2\pi} \sqrt{f_1(q)f_2(q)} \right) \\ &= N\epsilon_0 + \frac{N}{\beta\rho} \int_{BZ} \frac{d^2q}{(2\pi)^2} \log \left[\frac{\beta\Lambda^2}{2\pi} \sqrt{f_1(q)f_2(q)} \right],\end{aligned}\quad (25)$$

is the Helmholtz free energy for a generic quadratic model in terms of the interactions $f_1(q)$ and $f_2(q)$.

B. Self-consistent variational Bogoliubov approach

We start from the Bogoliubov inequality, which allow us to define the variational free energy as:

$$F \leq F_{var} = F_0 + \langle H \rangle_0 - \langle H_0 \rangle_0, \quad (26)$$

where the averages with zero sub-index are taken using the Boltzmann measure of the test model H_0 , chosen with the same functional form of eq. (23):

$$H_0 = N\epsilon_0 + \frac{1}{2} \left(\frac{\sqrt{3}a^2}{2} \right) \int_{BZ} \frac{d^2q}{(2\pi)^2} \left[f_1(\mathbf{q}) |\hat{u}_{\parallel}(\mathbf{q})|^2 + f_2(\mathbf{q}) |\hat{u}_{\perp}(\mathbf{q})|^2 \right], \quad (27)$$

where now the functions $f_1(\mathbf{q})$ and $f_2(\mathbf{q})$ should be adjusted in order to minimize the variational free energy. Considering the quadratic nature of test Hamiltonian of eq. (27), the deformation field correlation functions are given by:

$$\begin{aligned}\langle \hat{u}_{\parallel}(\mathbf{q}) \hat{u}_{\parallel}(\mathbf{q}') \rangle_0 &= \frac{(2\pi)^2 \delta(\mathbf{q} + \mathbf{q}')}{\frac{\sqrt{3}a^2}{2} \beta f_1(q)}, \\ \langle \hat{u}_{\perp}(\mathbf{q}) \hat{u}_{\perp}(\mathbf{q}') \rangle_0 &= \frac{(2\pi)^2 \delta(\mathbf{q} + \mathbf{q}')}{\frac{\sqrt{3}a^2}{2} \beta f_2(q)},\end{aligned}\quad (28)$$

and it is then straightforward to conclude that:

$$\langle H_0 \rangle_0 = N\epsilon_0 + \frac{1}{2} \left(\frac{\sqrt{3}a^2}{2} \right) \int \frac{d^2q}{(2\pi)^2} [f_1(\mathbf{q}) \langle |\hat{u}_{\parallel}(\mathbf{q})|^2 \rangle_0 + f_2(\mathbf{q}) \langle |\hat{u}_{\perp}(\mathbf{q})|^2 \rangle_0] = N\epsilon_0 + Nk_B T. \quad (29)$$

In order to complete the construction of the variational free energy, we now proceed to the calculus of $\langle H \rangle_0$. If we consider the translational symmetry of the solid phase is possible to write:

$$\langle H \rangle_0 = \frac{N}{2} \sum_{\mathbf{R}_i \neq \mathbf{0}} \langle V(\mathbf{R}_i + \mathbf{u}(\mathbf{R}_i) - \mathbf{u}(\mathbf{0})) \rangle_0 = \frac{N}{2} \sum_{\mathbf{R}_i \neq \mathbf{0}} \int \frac{d^2q}{(2\pi)^2} e^{i\mathbf{q} \cdot \mathbf{R}} g_{\mathbf{q}}(\mathbf{R}) \hat{V}(q), \quad (30)$$

where $\{\mathbf{R}_i\}$ represent the vectors of the triangular lattice at a given density, and $g_{\mathbf{q}}(\mathbf{R})$ is the positional correlation function.

Positional correlation function $g_{\mathbf{q}}(\mathbf{R})$

In the process of evaluating $\langle H \rangle_0$ we need to find the positional correlation function $g_{\mathbf{q}}(\mathbf{R}) = \langle e^{i\mathbf{q} \cdot (\mathbf{u}(\mathbf{R}) - \mathbf{u}(\mathbf{0}))} \rangle_0$, which in turn can be calculated as follows:

$$\begin{aligned} g_{\mathbf{q}}(\mathbf{R}) &= \exp -\frac{1}{2} \sum_{\alpha, \beta} q_{\alpha} q_{\beta} \langle (u_{\alpha}(\mathbf{R}) - u_{\alpha}(\mathbf{0}))(u_{\beta}(\mathbf{R}) - u_{\beta}(\mathbf{0})) \rangle_0 \\ &= \exp -\frac{1}{2} \sum_{\alpha, \beta} q_{\alpha} q_{\beta} \left(\frac{\sqrt{3}a^2}{2} \right)^2 \int \frac{d^2k d^2k'}{(2\pi)^2} (e^{i\mathbf{k} \cdot \mathbf{R}} - 1) (e^{i\mathbf{k}' \cdot \mathbf{R}} - 1) \langle u_{\alpha}(\mathbf{k}) u_{\beta}(\mathbf{k}') \rangle_0 \\ &= \exp -\frac{1}{2} \frac{\sqrt{3}a^2}{2} \int_{BZ} \frac{d^2k}{(2\pi)^2} 2(1 - \cos(\mathbf{k} \cdot \mathbf{R})) \left[\frac{(\mathbf{k} \cdot \mathbf{q})^2}{k^2} \langle |\hat{u}_{\parallel}(\mathbf{k})|^2 \rangle_0 + \frac{(\mathbf{k}_{\perp} \cdot \mathbf{q})^2}{k^2} \langle |\hat{u}_{\perp}(\mathbf{k})|^2 \rangle_0 \right] \\ &= \exp -\frac{1}{\beta\rho} \int_{BZ} \frac{d^2k}{(2\pi)^2} (1 - \cos(\mathbf{k} \cdot \mathbf{R})) \left[\frac{(\mathbf{k} \cdot \mathbf{q})^2}{k^2} \frac{1}{f_1(\mathbf{k})} + \frac{(\mathbf{k}_{\perp} \cdot \mathbf{q})^2}{k^2} \frac{1}{f_2(\mathbf{k})} \right]. \end{aligned} \quad (31)$$

At this point we can verify that in the limit of zero temperature ($\beta \rightarrow \infty$) the positional correlation function converge to one, as expected for the perfectly ordered crystal. For low temperatures, it is possible to prove that the leading order behavior of $f_1(\mathbf{k})$ and $f_2(\mathbf{k})$ agrees with the harmonic results given in Eqs. (23).

Calculation of $g_{\mathbf{q}}(\mathbf{R})$ considering the leading behavior of $f_1(\mathbf{k})$ and $f_2(\mathbf{k})$

Here we calculate $g_{\mathbf{q}}(\mathbf{R})$ considering that $f_1(\mathbf{k})$ and $f_2(\mathbf{k})$ are given by its low momentum quadratic behaviour, $f_1(\mathbf{k}) = r_1 k^2$ and $f_2(\mathbf{k}) = r_2 k^2$. This consideration lead us to:

$$g_{\mathbf{q}}(\mathbf{R}) = \exp -\frac{1}{\beta\rho} \int_{BZ} \frac{d^2k}{(2\pi)^2} (1 - \cos(\mathbf{k} \cdot \mathbf{R})) \left[\frac{(\mathbf{k} \cdot \mathbf{q})^2}{k^2} \frac{1}{r_1 k^2} + \frac{(\mathbf{k}_{\perp} \cdot \mathbf{q})^2}{k^2} \frac{1}{r_2 k^2} \right]. \quad (32)$$

To proceed it is convenient to write \mathbf{q} in a coordinate system in which the x-axis is taken along \mathbf{R} . This choice simplifies the algebraic manipulations to find r_1 and r_2 . Firstly, we can rewrite the scalar products in the above expression as

$$\begin{aligned} \mathbf{k} \cdot \mathbf{q} &= k_{\perp} q_{\perp} + k_{\parallel} q_{\parallel}, \\ \mathbf{k}_{\perp} \cdot \mathbf{q} &= -k_{\perp} q_{\parallel} + k_{\parallel} q_{\perp}. \end{aligned} \quad (33)$$

On this basis, Eq. (32) can be rewritten as

$$\begin{aligned} g_{\mathbf{q}}(\mathbf{R}) &= \exp -\frac{1}{\beta\rho} \int_{BZ} \frac{d^2k}{(2\pi)^2} \frac{1 - \cos(\mathbf{k} \cdot \mathbf{R})}{k^4} \left[\frac{k_{\perp}^2 q_{\perp}^2}{r_1} + \frac{2k_{\perp} q_{\perp} k_{\parallel} q_{\parallel}}{r_1} + \frac{k_{\parallel}^2 q_{\parallel}^2}{r_1} + \frac{k_{\perp}^2 q_{\parallel}^2}{r_2} - \frac{2k_{\perp} q_{\perp} k_{\parallel} q_{\parallel}}{r_2} + \frac{k_{\parallel}^2 q_{\perp}^2}{r_2} \right] \\ &\approx \exp -\frac{1}{\beta\rho} \left[\left(\frac{A_{\parallel}(\mathbf{R})}{r_1} + \frac{A_{\perp}(\mathbf{R})}{r_2} \right) q_{\parallel}^2 + \left(\frac{A_{\perp}(\mathbf{R})}{r_1} + \frac{A_{\parallel}(\mathbf{R})}{r_2} \right) q_{\perp}^2 \right] \\ &= \exp -\omega_{\parallel}(\mathbf{R}) q_{\parallel}^2 - \omega_{\perp}(\mathbf{R}) q_{\perp}^2, \end{aligned} \quad (34)$$

where the coefficients $\omega_{\parallel}(\mathbf{R})$ and $\omega_{\perp}(\mathbf{R})$ are given as:

$$\begin{aligned}\omega_{\parallel}(\mathbf{R}) &= \frac{1}{\beta\rho} \left(\frac{A_{\parallel}(\mathbf{R})}{r_1} + \frac{A_{\perp}(\mathbf{R})}{r_2} \right) \\ \omega_{\perp}(\mathbf{R}) &= \frac{1}{\beta\rho} \left(\frac{A_{\perp}(\mathbf{R})}{r_1} + \frac{A_{\parallel}(\mathbf{R})}{r_2} \right),\end{aligned}\quad (35)$$

and the functions $A_{\parallel}(\mathbf{R})$ and $A_{\perp}(\mathbf{R})$ are defined as the following integrals over the first Brillouin zone of the hexagonal crystal:

$$\begin{aligned}A_{\parallel}(\mathbf{R}) &= \int_{BZ} \frac{d^2k}{(2\pi)^2} \frac{1 - \cos(\mathbf{k} \cdot \mathbf{R})}{k^4} \frac{(\mathbf{k} \cdot \mathbf{R})^2}{R^2} \\ A_{\perp}(\mathbf{R}) &= \int_{BZ} \frac{d^2k}{(2\pi)^2} \frac{1 - \cos(\mathbf{k} \cdot \mathbf{R})}{k^4} \frac{(\mathbf{k} \cdot \mathbf{R}_{\perp})^2}{R^2}.\end{aligned}\quad (36)$$

Here it is important to notice that in the determination of $g_{\mathbf{q}}(\mathbf{R})$ we have neglected the cross term proportional to $q_{\parallel}q_{\perp}$ in the argument of the exponential function. This approximation is very well justified since, depending on the direction of \mathbf{R} , the corresponding coefficient is either zero, or a small and rapidly decreasing function of R whose highest value is of the order of 1% of the other coefficients in the quadratic form.

Variational free energy and the self-consistent harmonic approximation

Considering the obtained results for F_0 , $\langle H_0 \rangle_0$ and $\langle H \rangle_0$, we can now write the variational free energy per particle in units of $k_B T$ as:

$$\beta f_{var}[f_1(\mathbf{q}), f_2(\mathbf{q})] = \frac{1}{\rho} \int_{BZ} \frac{d^2q}{(2\pi)^2} \log \left[\frac{\beta\Lambda^2}{2\pi} \sqrt{f_1(\mathbf{q})f_2(\mathbf{q})} \right] - 1 + \frac{\beta}{2} \sum_{\mathbf{R}_j \neq \mathbf{0}} \int \frac{d^2q}{(2\pi)^2} e^{i\mathbf{q} \cdot \mathbf{R}_j} g_{\mathbf{q}}(\mathbf{R}_j) \hat{V}(q). \quad (37)$$

Demanding that $\delta f_{var}/\delta f_1(\mathbf{q}_0) = 0$ and $\delta f_{var}/\delta f_2(\mathbf{q}_0) = 0$, lead us to the following set of integral equations for $f_1(\mathbf{q})$ and $f_2(\mathbf{q})$:

$$\begin{aligned}f_1(\mathbf{q}_0) &= \sum_{\mathbf{R}_j \neq \mathbf{0}} (\cos(\mathbf{q}_0 \cdot \mathbf{R}_j) - 1) \int \frac{d^2q}{(2\pi)^2} e^{i\mathbf{q} \cdot \mathbf{R}_j} \hat{V}(q) g_{\mathbf{q}}(\mathbf{R}_j) \frac{(\mathbf{q}_0 \cdot \mathbf{q})^2}{q_0^2} \\ f_2(\mathbf{q}_0) &= \sum_{\mathbf{R}_j \neq \mathbf{0}} (\cos(\mathbf{q}_0 \cdot \mathbf{R}_j) - 1) \int \frac{d^2q}{(2\pi)^2} e^{i\mathbf{q} \cdot \mathbf{R}_j} \hat{V}(q) g_{\mathbf{q}}(\mathbf{R}_j) \frac{(\mathbf{q}_0^{\perp} \cdot \mathbf{q})^2}{q_0^2},\end{aligned}\quad (38)$$

where $\mathbf{q}_0 = (q_{0,x}, q_{0,y})$, $\mathbf{q}_0^{\perp} = (-q_{0,y}, q_{0,x})$ and $g_{\mathbf{q}}(\mathbf{R}_j)$ is given by Eq. (31). The numerical solution of this set of integral equations is a quite difficult task. However, since we are interested in the low momentum behavior of $f_1(\mathbf{q})$ and $f_2(\mathbf{q})$, we can follow a simplifying approach. Considering the symmetries of the solid phase under study, we already know that in the low momentum regime ($\mathbf{q} \rightarrow 0$) the leading order behavior of the functions $f_1(\mathbf{q})$ and $f_2(\mathbf{q})$ will be proportional to q^2 . This feature can be used to derive a system of equations for the effective elastic coefficients of the solid, defined as:

$$\begin{aligned}r_1 &= \frac{1}{2} \lim_{q \rightarrow 0} (\partial^2 f_1(q)/\partial q^2) \equiv 2\mu(T) + \lambda(T) \\ r_2 &= \frac{1}{2} \lim_{q \rightarrow 0} (\partial^2 f_2(q)/\partial q^2) \equiv \mu(T).\end{aligned}\quad (39)$$

In this way, considering the form of Eq. (38), we can conclude that the elastic coefficients satisfy the following set of equations:

$$\begin{aligned}r_1 &= -\frac{1}{2} \sum_{\mathbf{R}_i \neq \mathbf{0}} (\mathbf{e} \cdot \mathbf{R}_i)^2 \int \frac{d^2q}{(2\pi)^2} e^{i\mathbf{q} \cdot \mathbf{R}_i} \hat{V}(q) g_{\mathbf{q}}(\mathbf{R}_i) (\mathbf{e} \cdot \mathbf{q})^2, \\ r_2 &= -\frac{1}{2} \sum_{\mathbf{R}_i \neq \mathbf{0}} (\mathbf{e} \cdot \mathbf{R}_i)^2 \int \frac{d^2q}{(2\pi)^2} e^{i\mathbf{q} \cdot \mathbf{R}_i} \hat{V}(q) g_{\mathbf{q}}(\mathbf{R}_i) (\mathbf{e}_{\perp} \cdot \mathbf{q})^2,\end{aligned}\quad (40)$$

where \mathbf{e} can be taken as $(1, 0)$ and \mathbf{e}_{\perp} as $(0, 1)$. Once we have obtained an exact system of equations for r_1 and r_2 is natural to approximate $f_1(\mathbf{q})$ and $f_2(\mathbf{q})$ by its low momentum form in the calculus of $g_{\mathbf{q}}(\mathbf{R})$, which allows us to reach Eq. (34). In this way the obtained expression for $g_{\mathbf{q}}(\mathbf{R})$ allow us to close system of Eqs. (40) for $r_1(T)$ and $r_2(T)$, which can now be used to study the melting process at all densities and temperatures.

Application to the Gaussian-Core Model (GCM)

In the case of the GCM we can benefit of the Gaussian form of the potential and rewrite the self-consistency relations given in Eqs. (40) in the following explicit way:

$$\begin{aligned}
 r_1 &= -\frac{1}{2} \sum_{\mathbf{R}} (\mathbf{e} \cdot \mathbf{R})^2 \int \frac{d^2 q}{(2\pi)^2} e^{iq_{\parallel} R} \left(\pi e^{-\frac{q_{\parallel}^2 + q_{\perp}^2}{4}} \right) \left(e^{-\omega_{\parallel} q_{\parallel}^2 - \omega_{\perp} q_{\perp}^2} \right) \left(q_{\perp}^2 \frac{(\mathbf{e} \cdot \mathbf{R}_{\perp})^2}{R^2} + q_{\parallel}^2 \frac{(\mathbf{e} \cdot \mathbf{R})^2}{R^2} \right), \\
 &= -\sum_{\mathbf{R}} R_x^2 \frac{2R_y^2 (\frac{1}{4} + \omega_{\parallel})^2 - R_x^2 [R^2 - 2(\frac{1}{4} + \omega_{\parallel})] (\frac{1}{4} + \omega_{\perp})}{32R^2 (\frac{1}{4} + \omega_{\parallel})^{5/2} (\frac{1}{4} + \omega_{\perp})^{3/2}} e^{-\frac{R^2}{1+4\omega_{\parallel}}}, \\
 r_2 &= -\frac{1}{2} \sum_{\mathbf{R}} (\mathbf{e} \cdot \mathbf{R})^2 \int \frac{d^2 q}{(2\pi)^2} e^{iq_{\parallel} R} \left(\pi e^{-\frac{q_{\parallel}^2 + q_{\perp}^2}{4}} \right) \left(e^{-\omega_{\parallel} q_{\parallel}^2 - \omega_{\perp} q_{\perp}^2} \right) \left(q_{\perp}^2 \frac{(\mathbf{e} \cdot \mathbf{R})^2}{R^2} + q_{\parallel}^2 \frac{(\mathbf{e} \cdot \mathbf{R}_{\perp})^2}{R^2} \right), \\
 &= -\sum_{\mathbf{R}} R_x^2 \frac{2R_x^2 (\frac{1}{4} + \omega_{\parallel})^2 - R_y^2 [R^2 - 2(\frac{1}{4} + \omega_{\parallel})] (\frac{1}{4} + \omega_{\perp})}{32R^2 (\frac{1}{4} + \omega_{\parallel})^{5/2} (\frac{1}{4} + \omega_{\perp})^{3/2}} e^{-\frac{R^2}{1+4\omega_{\parallel}}}.
 \end{aligned} \tag{41}$$

The numerical calculation of the set of integrals that determine $A_{\parallel}(\mathbf{R})$ and $A_{\perp}(\mathbf{R})$ is needed to determine the values of $\omega_{\parallel}(\mathbf{R})$ and $\omega_{\perp}(\mathbf{R})$ for each \mathbf{R} . With this information at hand, the solution of the system of Eqs. (41) is now possible. For comparison, in Fig. (3), we show the behavior of r_1 and r_2 at zero and at the melting temperature as a function of the scaled density ρr_0^2 . We observe that the value of μ decreases with temperatures at all densities while $(2\mu + \lambda)$ displays a weak non-monotonical behavior with temperature. Also we should notice the discontinuity of the elastic coefficients at the melting temperature, as expected in KT like transitions. Finally, we can also observe the expected behavior of the transversal elastic coefficient (μ) as the density is increased for a system exhibiting a reentrant melting as the GCM.

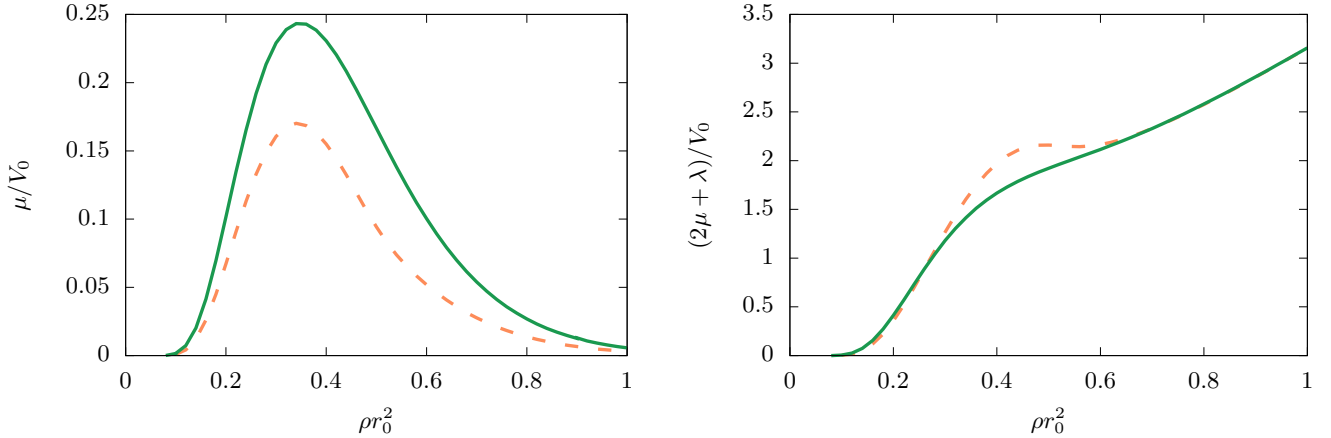


FIG. 3: Comparison of the Lamé coefficients at $T = 0$ and $T = T_m$. The solid curves represent the ground state values and the dashed lines represent the value at $T = T_m$.

C. Energy of dislocations and application of the RG theory

The Hamiltonian of a pair of interacting dislocations, defined on a certain periodic lattice, can be written in Fourier space as [26, 52]:

$$\frac{H_D}{k_B T} = \frac{-K}{8\pi} \frac{1}{(A_{uc})^2} \int_{BZ} \frac{d^2 q}{(2\pi)^2} \sum_{i,j} \hat{\mathbf{b}}_i(\mathbf{q}) \hat{\mathbf{b}}_j(-\mathbf{q}) \left(-\frac{4\pi}{q^2} \delta_{ij} + 4\pi \frac{q_i q_j}{q^4} \right), \tag{42}$$

where $K = \frac{4\mu(\mu+\lambda)}{(2\mu+\lambda)k_B T}$ is the Franck constant of the crystal in units of $k_B T$, $\hat{\mathbf{b}}(\mathbf{q})$ denote the Burger's vector density, A_{uc} represent the area of the unitary cell of the lattice and a represent the lattice spacing of the crystal. A dimensional analysis of this equation lead us to the conclusion that $\hat{\mathbf{b}}(\mathbf{q})$ has the same dimension of a^2 , this means that $\mathbf{b}(\mathbf{r})$ is dimensionless, which is naturally interpreted as $\mathbf{b}(\mathbf{r})$ been measured in units of a .

Let us consider that the density associated to the Burguer's vector of a dislocation at position \mathbf{R} of the discrete lattice is given by:

$$\mathbf{b}_d(\mathbf{r}, \mathbf{R}) = \mathbf{e} \delta_{\mathbf{r}, \mathbf{R}}. \quad (43)$$

where $\delta_{\mathbf{r}, \mathbf{R}}$ represent the standard Kronecker delta symbol and \mathbf{e} represent the Burguer's vector of the corresponding dislocation. Now we would like to extend the field defined in eq. (43) to the continuum to proceed with the calculation of the energy of a dislocation. Let us define this field as $\mathbf{b}_c(\mathbf{r})$. From dimensional arguments, it is natural to propose the following relation between both formulations:

$$\int_{uc(\mathbf{R})} \mathbf{b}_c(\mathbf{r}' - \mathbf{R}) d^2 \mathbf{r}' = A_{uc} \mathbf{b}_d(\mathbf{R}, \mathbf{R}), \quad (44)$$

where A_{uc} is taken as $\frac{1}{2}\sqrt{3}a^2$ considering that dislocations are located on the underlying triangular lattice of the solid. The previous relation lead us to the conclusion that $\mathbf{b}_c(\mathbf{r}) = \frac{1}{2}\sqrt{3}a^2 \mathbf{e} \delta(\mathbf{r})$. In this way the field corresponding to a conjugate dislocation pair — as the one shown in Fig. 4 — separated by a vector \mathbf{d} and oriented in the direction \mathbf{e} can be written as

$$\mathbf{b}_c(\mathbf{r}) = \frac{\sqrt{3}a^2}{2} [\delta(\mathbf{r} - \mathbf{d}/2) - \delta(\mathbf{r} + \mathbf{d}/2)] \mathbf{e}. \quad (45)$$

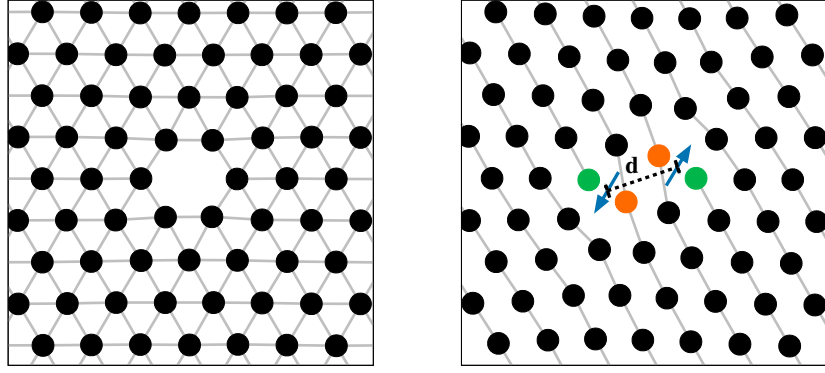


FIG. 4: Vacancy and conjugate dislocation pair in a triangular lattice. The particles in green has five neighbours and in orange has seven. The arrows represent the burgers vector of each dislocation.

The modulus of the vector \mathbf{e} is take it as one, which corresponds to the minimum possible value of the Burguer's vector of a dislocation in units of the lattice spacing. Now we can write our dislocation field in Fourier space as:

$$\hat{\mathbf{b}}(\mathbf{q}) = \frac{\sqrt{3}a^2}{2} (-2i) \sin\left(\frac{\mathbf{q} \cdot \mathbf{d}}{2}\right) \mathbf{e}, \quad (46)$$

It is not difficult to realize at this point that the energy of a dislocation pair will depend on the orientation of the vectors \mathbf{d} , parameterized by the angle α , and \mathbf{e} , parameterized by the angle θ , respect to the x -axis. Consequently, we observe that the x and y components of the dislocation density field are given by:

$$\begin{aligned} \hat{b}_x(\mathbf{q}) &= \frac{\sqrt{3}a^2}{2} (-2i) \cos(\theta) \sin\left(\frac{\mathbf{q} \cdot \mathbf{d}}{2}\right), \\ \hat{b}_y(\mathbf{q}) &= \frac{\sqrt{3}a^2}{2} (-2i) \sin(\theta) \sin\left(\frac{\mathbf{q} \cdot \mathbf{d}}{2}\right). \end{aligned} \quad (47)$$

The energy of a single dislocation can be written then as:

$$\begin{aligned} \frac{E_c}{k_B T} &= \frac{K}{8\pi} \frac{1}{(A_{uc})^2} \int_{BZ} \frac{d^2 q}{(2\pi)^2} \frac{4\pi}{q^2} \left[\hat{b}_x(\mathbf{q}) \hat{b}_x(-\mathbf{q}) \left(1 - \frac{q_x^2}{q^2}\right) + 2\hat{b}_x(\mathbf{q}) \hat{b}_y(-\mathbf{q}) \left(-\frac{q_x q_y}{q^2}\right) + \right. \\ &\quad \left. + \hat{b}_y(\mathbf{q}) \hat{b}_y(-\mathbf{q}) \left(1 - \frac{q_y^2}{q^2}\right) \right], \end{aligned} \quad (48)$$

which after some simplifications can be cast in the following form

$$\begin{aligned} \frac{E_c}{k_B T} &= \frac{K}{16\pi} \frac{1}{A_{uc}^2} \int_{BZ} \frac{d^2 q}{(2\pi)^2} \frac{12\pi a^4 (\mathbf{q}_\perp \cdot \mathbf{e})^2}{q^4} \sin^2(\mathbf{q} \cdot \mathbf{d}/2), \\ &= K \int_{BZ} \frac{d^2 q}{(2\pi)^2} \frac{(\mathbf{q}_\perp \cdot \mathbf{e})^2}{q^4} \sin^2(\mathbf{q} \cdot \mathbf{d}/2). \end{aligned} \quad (49)$$

To finally determine the actual value of the energy of a dislocation, we take the arithmetic average over all possible configurations in θ and α , considering the do not have in fact one single type of defect but a continuous class. This procedure allow us to conclude that:

$$\begin{aligned} \langle (\mathbf{q}_\perp \cdot \mathbf{e})^2 \rangle_\theta &= \frac{q^2}{2}, \\ \langle \sin^2(\mathbf{q} \cdot \mathbf{d}/2) \rangle_\alpha &= \frac{1}{2} (1 - J_0(qd)), \end{aligned} \quad (50)$$

leading us to the result:

$$\frac{E_c}{k_B T} = K \int_{BZ} \frac{d^2 q}{(2\pi)^2} \frac{1 - J_0(qd)}{4q^2}. \quad (51)$$

In order to estimate the core energy of a defect, we need as an input the distance between the dislocations d . We can consider this distance as the minimum distance for which a dislocation pair is stable, since such pairs are the most relevant.

Finally we should observe that we still need to estimate the value of the average minimum distance between dislocations (d) in stable configurations. To understand better how to estimate such a quantity we performed M.D. simulations at $k_B T \sim 0$ (see Supp. Mat. D) for the specific model under consideration (GCM). We used the ordered triangular lattice as initial condition for our simulation and removed or added a single particle. This vacancy or interstitial defects can be both considered as dislocation pairs, but we often regard them as different kind of defects, since they have higher symmetry [54]. In our simulations we have noticed that vacancies are stable for $\rho \leq 0.3$, and naturally small fluctuations continuously deform its structure into pairs of dislocations with distance $d \sim \sqrt{3}a$ for $\rho > 0.3$ – both cases are represented in Fig. 4.

For higher temperatures, we have also noticed the presence of dislocation pairs more tightly bounded. Different from the defects found by relaxing the system from a vacancy initial condition, these pairs are not stable. They can be thus thought as “virtual” dislocation pairs, as they vanish quickly if we let the system relax at $k_B T \sim 0$. As an example of this line of reasoning, in ref. [54], defects are considered as dislocation pairs only if the separation is greater than a certain threshold value necessarily higher than the lattice spacing of the underlying lattice.

Finally, if we consider $d = \sqrt{3}a$ in Eq. (51) and perform the numeric integration over the Brillouin zone, we can conclude our estimate that $E_c/k_B T = bK$, with $b \simeq 0.072$.

D. Numerical simulations

In order to confront the phase diagram found by us, we have performed simulations of the GCM in a NVT ensemble. Previous simulation results for this model are available in the NPT ensemble [51]. We are interested in sampling the equilibrium configurations, so we have used the Langevin equation in the overdamped limit to simulate the behavior of the system in contact with a heat bath:

$$\gamma \dot{\mathbf{r}}_i = - \sum_j \nabla_i V(|\mathbf{r}_i - \mathbf{r}_j|) + \sqrt{2k_B T \gamma} \xi_i(t), \quad (52)$$

where T is the temperature of the thermal bath and γ is the viscosity. We can measure timescales in units of γ and temperature scales in units of V_0/k_B . The random forcing $\xi_i(t)$ is a white noise with $\langle \xi_i(t) \rangle = 0$ and $\langle \xi_i(t) \xi_j(t') \rangle = \delta_{ij} \delta(t - t')$.

In order to integrate the N stochastic differential equations we use the Heun algorithm, equivalent to RK2 in the deterministic case [60, pg.192]. We have used a time step of $dt/\gamma = 0.1$ and a cutoff radius $r_c = 2.5a$, where a is the lattice parameter. We have also avoided the discontinuity at r_c by shifting the potential function by $V(r_c)$ [61, pg.145]. To thermalize the system efficiently for all temperatures, including those close to the transition temperatures, we have used a MPI implementation of the parallel tempering technique [62–64]. The choice of the distribution of temperatures in the parallel tempering is of a Gaussian distribution approximately centered in the middle of the hexatic phase. We have also used sets of two initial conditions, a liquid (disordered) and a crystalline (triangular lattice using $a = (2/\sqrt{3}\rho)^{1/2}$ as spacing), in order to define a criteria for the thermal equilibrium in each temperature.

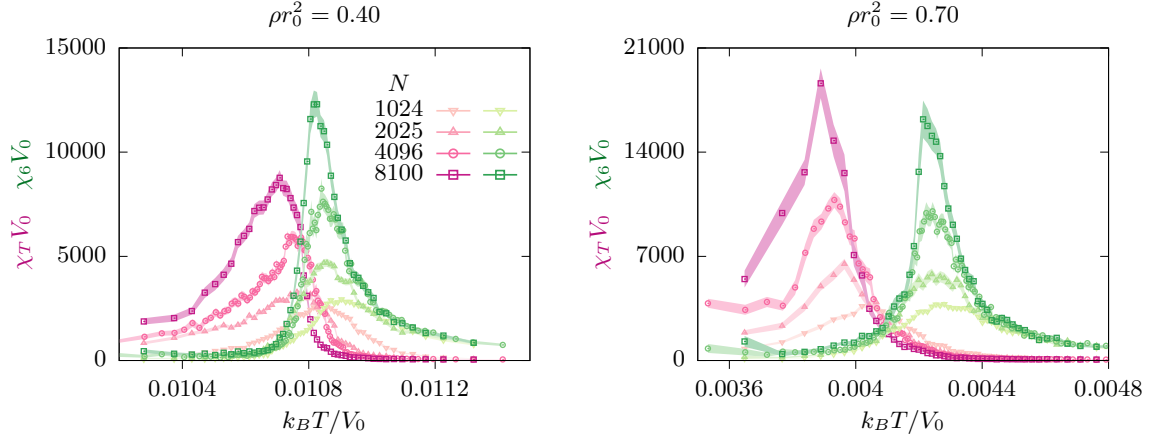


FIG. 5: Susceptibilities of order parameters for four different number of particles. We represent the susceptibilities of translational order parameter (χ_T) in magenta and susceptibilities of orientational order parameter (χ_6) in green. The width of the filled curves represent the statistical uncertainty of the data.

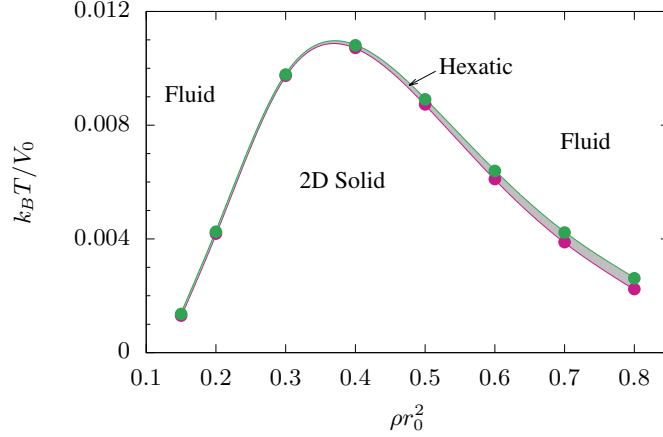


FIG. 6: Phase diagram of the Gaussian Core Model found by simulations in NVT ensemble. The points in green are the estimates for the hexatic-liquid transition and points in magenta are the estimates for the 2D solid-hexatic transition. The lines are guides to the eyes. The size of the hexatic phase is very small, and increases with the density for $\rho r_0^2 > 0.4$.

We have estimated the two melting temperatures, the first corresponding to the transition from the 2D solid phase to the hexatic phase, and the second from the hexatic to liquid phases, by measuring the related order parameters [9]. They are given by the following:

$$\Psi_T = \frac{1}{N} \left| \sum_j e^{i\mathbf{k}_0 \cdot \mathbf{r}_j} \right|, \quad (53)$$

$$\Psi_6 = \frac{1}{N} \left| \sum_j \frac{1}{NN(j)} \sum_l e^{6i\theta_{jl}} \right|, \quad (54)$$

where ψ_T is the translational and ψ_6 the orientational order parameters, \mathbf{k}_0 is the characteristic vector of the reciprocal lattice — determined by measuring the maximum of the structure factor —, $NN(j)$ is the nearest neighbours of the particle j and θ_{jl} is the bond angle between particles j and l — both determined by a Delaunay triangulation. The signatures of the transitions are more evident in the corresponding order parameter susceptibilities:

$$\chi \equiv \frac{1}{k_B} \frac{\partial \Psi}{\partial T} = \frac{N}{k_B T} \left[\langle \Psi^2 \rangle - \langle \Psi \rangle^2 \right]. \quad (55)$$

In order to estimate the 2D solid melting temperature we observed the maximum of the translational order parameter susceptibility (χ_T), whereas for the hexatic melting temperature, the maximum of orientational order parameter susceptibility (χ_6). These quantities are shown as a function of temperature in Fig. 5 for an increasing number of particles and for two values of the density. The corresponding melting temperatures are estimated by extrapolating linearly the location of the maxima as a function of \sqrt{N}^{-1} . The resulting phase diagram is shown in Fig. 6.

* Electronic address: alejandro.mendoza@ufsc.br

- [1] R. Peierls. Quelques propriétés typiques des corps solides. *Annales de l'institut Henri Poincaré*, 5(3):177–222, 1935.
- [2] L. D. Landau. On the theory of phase transitions II. *Zh. Eksp. Teor. Fiz.*, 7:627, 1937.
- [3] N. D. Mermin and H. Wagner. Absence of Ferromagnetism or Antiferromagnetism in One- or Two-Dimensional Isotropic Heisenberg Models. *Physical Review Letters*, 17(22):1133–1136, November 1966.
- [4] P. C. Hohenberg. Existence of Long-Range Order in One and Two Dimensions. *Physical Review*, 158(2):383–386, June 1967.
- [5] V. L. Berezinskii. Destruction of Long-Range Order in One-Dimensional and Two-Dimensional Systems Having a Continuous Symmetry Group I. Classical Systems. *Sov.Phys.JETP*, page 8, 1971.
- [6] J. M. Kosterlitz and D. J. Thouless. Ordering, metastability and phase transitions in two-dimensional systems. *Journal of Physics C: Solid State Physics*, 6(7):1181–1203, April 1973.
- [7] Katherine J. Strandburg. Two-dimensional melting. *Reviews of Modern Physics*, 60(1):161–207, January 1988.
- [8] A.G. Naumovets, A.G. Lyuksyutov, and V. Pokrovsky. *Two-Dimensional Crystals*. Academic Press, 1992.
- [9] C. D.R. Nelson, Domb, M.S. Green, and J.L. Lebowitz. *Defect-Mediated Phase Transitions*, volume 7 of *Phase Transitions and Critical Phenomena*. Academic Press, 1983.
- [10] P.G. de Gennes and J. Prost. *The Physics of Liquid Crystals*. International series of monographs on physics. Clarendon Press, 1993.
- [11] D.R. Nelson. *Defects and Geometry in Condensed Matter Physics*. Cambridge University Press, 2002.
- [12] Daniel G. Barci, Alejandro Mendoza-Coto, and Daniel A. Stariolo. Nematic phase in stripe-forming systems within the self-consistent screening approximation. *Phys. Rev. E*, 88:062140, Dec 2013.
- [13] Alejandro Mendoza-Coto, Daniel A. Stariolo, and Lucas Nicolao. Nature of long-range order in stripe-forming systems with long-range repulsive interactions. *Phys. Rev. Lett.*, 114:116101, Mar 2015.
- [14] Alejandro Mendoza-Coto, Daniel G. Barci, and Daniel A. Stariolo. Quantum and thermal melting of stripe forming systems with competing long-range interactions. *Phys. Rev. B*, 95:144209, Apr 2017.
- [15] Alice L. Thorneywork, Joshua L. Abbott, Dirk G. A. L. Aarts, and Roel P. A. Dullens. Two-dimensional melting of colloidal hard spheres. *Phys. Rev. Lett.*, 118:158001, Apr 2017.
- [16] Ar. Abanov, V. Kalatsky, V. L. Pokrovsky, and W. M. Saslow. Phase diagram of ultrathin ferromagnetic films with perpendicular anisotropy. *Phys. Rev. B*, 51:1023–1038, Jan 1995.
- [17] Alejandro Mendoza-Coto, Danilo Emanuel Barreto de Oliveira, Lucas Nicolao, and Rogelio Díaz-Méndez. Topological phase diagrams of the frustrated Ising ferromagnet. *Physical Review B*, 101(17):174438, May 2020.
- [18] Ping Huang, Thomas Schönenberger, Marco Cantoni, Lukas Heinen, Arnaud Magrez, Achim Rosch, Fabrizio Carbone, and Henrik M. Rønnow. Melting of a skyrmion lattice to a skyrmion liquid via a hexatic phase. *Nature Nanotechnology*, 15(9):761–767, Sep 2020.
- [19] Christos N. Likos. Soft matter with soft particles. *Soft Matter*, 2(6):478, 2006.
- [20] M. A Glaser, G. M Grason, R. D Kamien, A Košmrlj, C. D Santangelo, and P Zihlerl. Soft spheres make more mesophases. *Europhysics Letters (EPL)*, 78(4):46004, may 2007.
- [21] I. Guillamón, H. Suderow, A. Fernández-Pacheco, J. Sesé, R. Córdoba, J. M. De Teresa, M. R. Ibarra, and S. Vieira. Direct observation of melting in a two-dimensional superconducting vortex lattice. *Nature Physics*, 5(9):651–655, Sep 2009.
- [22] Rogelio Díaz-Méndez, Fabio Mezzacapo, Wolfgang Lechner, Fabio Cinti, Egor Babaev, and Guido Pupillo. Glass Transitions in Monodisperse Cluster-Forming Ensembles: Vortex Matter in Type-1.5 Superconductors. *Physical Review Letters*, 118(6):067001, February 2017.
- [23] Indranil Roy, Surajit Dutta, Aditya N. Roy Choudhury, Somak Basistha, Ilaria Maccari, Soumyajit Mandal, John Jesudasan, Vivas Bagwe, Claudio Castellani, Lara Benfatto, and Pratap Raychaudhuri. Melting of the vortex lattice through intermediate hexatic fluid in an a-MoGe thin film. *Phys. Rev. Lett.*, 122:047001, Jan 2019.
- [24] V. L. Berezinsky. Destruction of long range order in one-dimensional and two-dimensional systems having a continuous symmetry group. I. Classical systems. *Sov. Phys. JETP*, 32:493–500, 1971.
- [25] David R. Nelson. Study of melting in two dimensions. *Phys. Rev. B*, 18:2318–2338, Sep 1978.
- [26] David R. Nelson and B. I. Halperin. Dislocation-mediated melting in two dimensions. *Physical Review B*, 19(5):2457–2484, March 1979.
- [27] S. Ostlund and B. I. Halperin. Dislocation-mediated melting of anisotropic layers. *Phys. Rev. B*, 23:335–358, Jan 1981.
- [28] A. P. Young. Melting and the vector coulomb gas in two dimensions. *Phys. Rev. B*, 19:1855–1866, Feb 1979.
- [29] John Toner and David R. Nelson. Smectic, cholesteric, and Rayleigh-Benard order in two dimensions. *Physical Review B*, 23(1):316–334, January 1981.
- [30] J Michael Kosterlitz. Kosterlitz–thouless physics: a review of key issues. *Reports on Progress in Physics*, 79(2):026001, jan 2016.
- [31] Sebastian C. Kapfer and Werner Krauth. Two-Dimensional Melting: From Liquid-Hexatic Coexistence to Continuous Transitions. *Physical Review Letters*, 114(3):035702, January 2015.
- [32] Etienne P. Bernard and Werner Krauth. Two-Step Melting in Two Dimensions: First-Order Liquid-Hexatic Transition. *Physical Review*

Letters, 107(15):155704, October 2011.

- [33] Yan-Wei Li and Massimo Pica Ciamarra. Attraction Tames Two-Dimensional Melting: From Continuous to Discontinuous Transitions. *Physical Review Letters*, 124(21):218002, May 2020.
- [34] Yan-Wei Li and Massimo Pica Ciamarra. Phase behavior of Lennard-Jones particles in two dimensions. *Physical Review E*, 102(6):062101, December 2020.
- [35] L. Benfatto, C. Castellani, and T. Giamarchi. Kosterlitz-thouless behavior in layered superconductors: The role of the vortex core energy. *Phys. Rev. Lett.*, 98:117008, Mar 2007.
- [36] I. Maccari, N. Defenu, L. Benfatto, C. Castellani, and T. Enss. Interplay of spin waves and vortices in the two-dimensional xy model at small vortex-core energy. *Phys. Rev. B*, 102:104505, Sep 2020.
- [37] Zhigang Wu, Jens K. Block, and Georg M. Bruun. Liquid crystal phases of two-dimensional dipolar gases and Berezinskii-Kosterlitz-Thouless melting. *Scientific Reports*, 6(1):19038, Jan 2016.
- [38] Nicolò Defenu, Andrea Trombettoni, István Nándori, and Tilman Enss. Nonperturbative renormalization group treatment of amplitude fluctuations for $|\varphi|^4$ topological phase transitions. *Phys. Rev. B*, 96:174505, Nov 2017.
- [39] A. Colcelli, N. Defenu, G. Mussardo, and A. Trombettoni. Finite temperature off-diagonal long-range order for interacting bosons. *Physical Review B*, 102(18), nov 2020.
- [40] Guido Giachetti, Nicolò Defenu, Stefano Ruffo, and Andrea Trombettoni. Self-consistent harmonic approximation in presence of non-local couplings(a). *Europhysics Letters*, 133(5):57004, March 2021.
- [41] Guido Giachetti, Andrea Trombettoni, Stefano Ruffo, and Nicolò Defenu. Berezinskii-Kosterlitz-Thouless transitions in classical and quantum long-range systems. *Physical Review B*, 106(1):014106, July 2022.
- [42] V. N. Ryzhov and E. E. Tareyeva. Two-stage melting in two dimensions: First-principles approach. *Phys. Rev. B*, 51:8789–8794, Apr 1995.
- [43] S. van Teeffelen, C. N Likos, N Hoffmann, and H Löwen. Density functional theory of freezing for soft interactions in two dimensions. *Europhysics Letters (EPL)*, 75(4):583–589, aug 2006.
- [44] Mengjie Zu, Jun Liu, Hua Tong, and Ning Xu. Density affects the nature of the hexatic-liquid transition in two-dimensional melting of soft-core systems. *Phys. Rev. Lett.*, 117:085702, Aug 2016.
- [45] Joshua A. Anderson, James Antonaglia, Jaime A. Millan, Michael Engel, and Sharon C. Glotzer. Shape and symmetry determine two-dimensional melting transitions of hard regular polygons. *Phys. Rev. X*, 7:021001, Apr 2017.
- [46] Jialing Guo, Yunhuan Nie, and Ning Xu. Signatures of continuous hexatic–liquid transition in two-dimensional melting. *Soft Matter*, 17:3397–3403, 2021.
- [47] Shubhendu Shekhar Khali, Dipanjan Chakraborty, and Debasish Chaudhuri. Two-step melting of the weeks–chandler–anderson system in two dimensions. *Soft Matter*, 17:3473–3485, 2021.
- [48] Óscar Toledano, M. Pancorbo, J. E. Alvarelos, and Óscar Gálvez. Melting in two-dimensional systems: Characterizing continuous and first-order transitions. *Phys. Rev. B*, 103:094107, Mar 2021.
- [49] A Lang, C N Likos, M Watzlawek, and H Löwen. Fluid and solid phases of the Gaussian core model. *Journal of Physics: Condensed Matter*, 12(24):5087–5108, June 2000.
- [50] Frank H. Stillinger and Thomas A. Weber. Gaussian core model in two dimensions. I. Melting transition. *The Journal of Chemical Physics*, 74(7):4015–4019, April 1981.
- [51] Santi Prestipino, Franz Saija, and Paolo V. Giaquinta. Hexatic Phase in the Two-Dimensional Gaussian-Core Model. *Physical Review Letters*, 106(23):235701, June 2011.
- [52] B. I. Halperin and David R. Nelson. Theory of Two-Dimensional Melting. *Physical Review Letters*, 41(2):121–124, July 1978.
- [53] See Supplemental Material at <http://link.aps.org/supplemental/> for details about (section A) the harmonic theory for solid elasticity and the derivation of the free energy of the Gaussian model Eq. (5); (section B) the determination of the functional form of the positional correlation function Eq. (31) and the set of equations for r_1 and r_2 , as well as the form of $g_{\mathbf{q}}(\mathbf{R})$ considering the harmonic approximation for $f_1(\mathbf{q})$ and $f_2(\mathbf{q})$ and the construction of the specific set of equations for r_1 and r_2 for the GCM; (section C) the estimation of the energy of a stable dislocation pair for GCM; (section D) the numerical simulations and the estimation of the 2D solid and hexatic melting temperatures.
- [54] Daniel S. Fisher, B. I. Halperin, and R. Morf. Defects in the two-dimensional electron solid and implications for melting. *Physical Review B*, 20(11):4692–4712, December 1979.
- [55] Alejandro Mendoza-Coto, Lucas Nicolao, and Rogelio Díaz-Méndez. On the mechanism behind the inverse melting in systems with competing interactions. *Scientific Reports*, 9:2020, 2019.
- [56] Daniel G. Barci, Alejandro Mendoza-Coto, and Daniel A. Stariolo. Nematic phase in stripe-forming systems within the self-consistent screening approximation. *Phys. Rev. E*, 88:062140, Dec 2013.
- [57] Alejandro Mendoza-Coto and Daniel A. Stariolo. Coarse-grained models of stripe forming systems: Phase diagrams, anomalies, and scaling hypothesis. *Phys. Rev. E*, 86:051130, Nov 2012.
- [58] R. Díaz-Méndez, A. Mendoza-Coto, R. Mulet, L. Nicolao, and D.A. Stariolo. Dynamics of systems with isotropic competing interactions in an external field: a langevin approach. *The European Physical Journal B*, 81:309–319, 2011.
- [59] Lucas Nicolao and Daniel A. Stariolo. Langevin simulations of a model for ultrathin magnetic films. *Phys. Rev. B*, 76:054453, Aug 2007.
- [60] T. C. Gard. *Introduction to Stochastic Differential Equations*. Number 114 in Monographs and Textbooks in Pure and Applied Mathematics. M. Dekker, New York, 1988.
- [61] M. P. Allen and D. J. Tildesley. *Computer Simulation of Liquids*. Clarendon Press, 1987.
- [62] Koji Hukushima and Koji Nemoto. Exchange monte carlo method and application to spin glass simulations. *Journal of the Physical Society of Japan*, 65(6):1604–1608, 1996.
- [63] E Marinari and G Parisi. Simulated Tempering: A New Monte Carlo Scheme. *Europhysics Letters (EPL)*, 19(6):451–458, July 1992.
- [64] Yuji Sugita and Yuko Okamoto. Replica-exchange molecular dynamics method for protein folding. *Chemical Physics Letters*, 314(1-

2):141–151, November 1999.

- [65] Within the KTHNY theory, it is well established that the effective Franck constant at the critical point $K(l \rightarrow \infty)$ is equal to 16π . However the corresponding value of the bare Franck constant $K(0)$ it is not an universal quantity and its value at the critical point depends on the specific energy cost of the relevant defects. Within our framework, this value is given by $K(0)_c \approx 23.922\pi$.